

Foraging by Deep-Diving Birds Is Not Constrained by an Aerobic Diving Limit: A Model of Avian Depth-Dependent Diving Metabolic Rate

Erpur Snær Hansen* and Robert E. Ricklefs

Department of Biology, University of Missouri, St. Louis, Missouri
63121-4499

Submitted March 19, 2003; Accepted September 24, 2003;
Electronically published February 27, 2004

Online enhancements: appendixes, table, color figures.

ABSTRACT: The theoretical aerobic diving limit (tADL) specifies the duration of a dive after which oxygen reserves available for diving are depleted. The tADL has been calculated by dividing the available oxygen stores by the diving metabolic rate (DMR). Contrary to diving mammals, most diving birds examined to date exceed the tADL by a large margin. This discrepancy between observation and theory has engendered two alternative explanations suggesting that dive duration is extended either anaerobically or by depressing aerobic metabolism. Current formulations of tADL uncritically assume that DMR is independent of depth. However, diving birds differ from other vertebrate divers by having a larger respiratory system volume and by retaining air in their plumage while diving, thereby elevating buoyancy. Because air compresses with depth, diving power requirement decreases with depth. Following this principle, we modeled DMR to depth for Adelic and little penguins and reformulated the tADL accordingly. The model's results suggest that $< \sim 5\%$ of natural dives by Adelic penguins exceed the reformulated tADL(d), or maximal aerobic depth, and none in the more buoyant little penguin. These data suggest that, for both small and large species, deep diving birds rarely if ever exceed tADL(d).

Keywords: diving metabolic rate, aerobic diving limit, oxygen reserves, buoyancy, foraging constraints, penguins.

The most important aspects of the physiological and metabolic processes dictating diving in air-breathing homeothermic endotherms are the oxygen storage capacity

* Corresponding author. Present address: Háaleitisbraut 109, 108 Reykjavík, Iceland; e-mail: erpur@hi.is.

Am. Nat. 2004. Vol. 163, pp. 358–374. © 2004 by The University of Chicago. 0003-0147/2004/16303-30108\$15.00. All rights reserved.

and the rate of oxygen consumption. The combination of these two factors is summarized descriptively by the aerobic diving limit (ADL). The ADL is defined as the maximum period of breath holding that does not result in an increase in blood lactic acid concentration during or after a dive (Kooyman et al. 1983). If dives consistently exceeded ADL, the accumulation of lactic acid would result in progressive, exponential lengthening of the postdive pauses or, depending on the extent, a suspension of diving until normal lactate levels were reestablished (Kooyman 1989).

Postdiving plasma lactate levels of birds have been measured only twice, in both instances in the laboratory (Stephenson et al. 1992; Ponganis et al. 1997), and because of the practical difficulty of measurement, especially in relatively small-bodied animals such as birds, the situation is not likely to improve much. This has led to the substitution in diving studies of a calculated ADL (cADL), also termed "theoretical" (tADL) in the literature (Kooyman and Kooyman 1995), the latter notation being followed here. The tADL is the time available until oxygen reserves are depleted, and it is calculated by dividing the available oxygen stores (mL O_2) by the diving metabolic rate ($\text{DMR; mL O}_2 \text{ s}^{-1}$). In many studies, observed dive times exceed the tADL, sometimes by a considerable amount. Most notable is the ability of Weddell seals to dive three times longer than their measured ADL determined by postdive lactate levels. The heart and central nervous system, which are sensitive to low oxygen levels, must therefore be supplied for longer than other tissues, implying that ADL is not really an abrupt phenomenon (as simplistically implied in the tADL definition) but a transitional process. A critical assumption in the calculation of tADL is that DMR is constant and independent of depth. This article demonstrates for positively buoyant birds that DMR decreases with depth because of reduced buoyancy resulting from compression of air in the respiratory system and feathers and that depth-dependent DMR largely explains the discrepancy between observed (bADL) and expected tADL.

Most species of avian divers that have been examined, penguins in particular, consistently surpass the tADL, commonly by a wide margin (Kooyman 1975, 1989; Croll 1990; Croll et al. 1992; Kooyman et al. 1992; Chappell et al. 1993a, 1993b; Croll and McLaren 1993; Kooyman and Kooyman 1995; Wilson 1995; Boyd and Croxall 1996). However, in most of these studies, the postdive pauses that follow dives surpassing the tADL in duration do not exceed those following "aerobic" dives ($<tADL$) and do not lengthen over a series of dives, as expected for dives surpassing the ADL. Exceptions occur only after rare dives exceeding the tADL by a large margin (e.g., Ydenberg and Guillemette 1991; Croll and McLaren 1993). This discrepancy between observation and tADL has generated a behavioral definition of the ADL (bADL), which assumes that only those dives followed by extended postdive pauses exceed the ADL (Kooyman and Kooyman 1995).

The common absence of extended pauses after dives that greatly exceed tADL and the large discrepancy between the tADL and bADL when postdive pauses do lengthen (e.g., Culik et al. 1998; Luna-Jorquera and Culik 2000) has engendered two currently competing explanations (Boyd 1997). The first explanation states that dive duration is anaerobically extended. The second states that dive duration is extended by depressing aerobic metabolism (Kooyman 1989; Boyd 1997) by reducing blood flow to peripheral tissues (Stephenson and Jones 1992), possibly supplemented by localized hypothermia (Wilson and Grémillet 1996; Bevan et al. 1997; Handrich et al. 1997). This hypometabolism hypothesis is generally considered better supported by a diverse body of evidence (Mill and Baldwin 1983; Davis and Guderley 1987, 1990; Boyd 1997; Butler and Jones 1997; Kovacs and Meyers 2000).

A neglected third possibility is that the tADL assumptions are incorrect (Boyd and Croxall 1996) because oxygen reserves are underestimated, diving metabolic rate is overestimated, or both. Although all components of oxygen storage capacity have been evaluated for only a few avian species, the measurements and assumptions involved are nevertheless considered fairly robust (Kooyman 1989; but see Ponganis et al. 1993). In contrast, DMR has never been measured directly in free-ranging birds. The DMR values used in tADL calculations come from laboratory measurements (Butler and Woakes 1984; Baudinette and Gill 1985; Hui 1988; Croll and McLaren 1993; Culik et al. 1994b, 1996; Luna-Jorquera and Culik 2000) and from time-partitioned field metabolic rates (FMR; Nagy et al. 1984; Kooyman et al. 1992; Chappell et al. 1993a). Excluding an outlier from Nagy et al. (1984), these DMR values lie within the range of two to four times the standard metabolic rate (Kooyman 1989). No laboratory study to date has measured the oxygen consumption of a diving bird at a depth greater than a few meters. Furthermore, the time-partitioned FMR studies

cited above equate "FMR at sea" with DMR. The "FMR at sea" results from time allocations to various activities (diving, swimming, resting, and flying) that differ in their average metabolic costs and therefore by definition cannot represent DMR, a point also made by Bevan et al. (1995).

The assumption that DMR is constant and independent of depth has received relatively little discussion in the literature (but see Wilson et al. 1992; Clowater and Burger 1994). It is well known, however, that birds differ from mammals in having an approximately three times larger respiratory system air volume (at 1 kg; Calder 1984) in addition to the plumage air and that buoyancy is far more important than drag in determining the energy cost of diving in shallow divers (Stephenson et al. 1989a; Lovvorn 1991). The theoretical consequences of this "air cargo" on diving metabolic rate at depth are examined in this article to determine whether they explain why birds systematically exceed conventionally calculated tADL. This approach is based on evaluating the reduction in air volume with depth, which follows Boyle's Law (Wilson et al. 1992; Webb et al. 1998; Skrovan et al. 1999; Williams et al. 2000; Davis et al. 2001; Nowacek et al. 2001). Reduced air volume decreases both buoyancy and body surface area at depth, the latter determining parasite body drag. Depth-dependent body volume (and surface) are used here to calculate depth-dependent DMR, $DMR(d)$, which in turn is used to calculate a depth-dependent ADL, $tADL(d)$. Variables and parameters are compiled from the literature for the best-known avian diver in this context, the Adelie penguin (*Pygoscelis adeliae*). The model's results show that the magnitude of $DMR(d)$ reduction is sufficient alone, that is, without taking hypometabolism into account, to reconcile observed dive times with the tADL. Accordingly, fewer than ~4% of dives by Adelie penguins (field data from Chappell et al. 1993a) are likely to be anaerobic. To expand the scope of the model with respect to body size, an identical model of the more buoyant little penguin (*Eudyptula minor*) was constructed and compared to field data (Gales et al. 1990; Bethge et al. 1997). No dives by little penguins are likely to be anaerobic.

Basic Assumptions and Parameters

Body Volume

The air volume of diving birds is composed of plumage air (V_p) and respiratory system volume (V_r ; Calder 1984). It is assumed that V_r is augmented from the anecdotally observed habit of deep-diving birds to dive after inspiration (Kooyman et al. 1971; Stephenson et al. 1989b; Croll et al. 1992), but see "Discussion" for the case of shallow divers/diving.

The total volume of an Adelie penguin at the surface

is $V_O = V_b + V_R + V_p$ (see eq. [6]), where V_b is solid body volume. The $V_b = M_b/\tau$, where τ is solid body density, $1,065 \text{ kg m}^{-3}$ (Stephenson 1993). Thus, $V_b = 3.756 \times 10^{-3} \text{ m}^3$. The V_R is calculated by equation (1) (Calder 1984), where M_b is body mass:

$$V_R = 1.55 \times 10^{-4} M_b^{0.92} = 5.55 \times 10^{-4} \text{ m}^3. \quad (1)$$

The V_p at the surface was calculated by an ellipsoid volume subtraction. The method assumes that the bird's "inner core" volume (V_i) is roughly ellipsoid shaped, the volume of which is

$$V = \left(\frac{4}{3}\right)\pi ab^2, \quad (2)$$

where a is the semimajor axis (m), and b is the semiminor axis (m). The inner core constitutes the solid body volume and the total respiratory volume (m^3):

$$V_i = V_b + V_R = 4.324 \times 10^{-3} \text{ m}^3. \quad (3)$$

The outer core's semiminor axis (b_o) at the sea surface is the radius of the bird's thickest cross-sectional area, called "frontal body area," A_f (0.02083 m^2 ; Bannasch 1995):

$$b_o = \sqrt{\frac{A_f}{\pi}} = 0.0814 \text{ m}. \quad (4)$$

Ptilosuppression and water pressure were taken into account by assuming that the plumage layer thickness (f) is $5 \times 10^{-3} \text{ m}$ when just submerged as found by Kooyman et al. (1973). The outer core's semiminor axis minus the plumage layer thickness gives the inner core semiminor axis (b_i), $b_i = b_o - f$, or 0.0765 m . The inner core's semimajor axis at the surface, a_s , is

$$a_s = \frac{3}{4} \left(\frac{V_i}{\pi b_i^2} \right) = 0.1765 \text{ m}. \quad (5)$$

The outer core's semimajor axis (a_o) is $a_o = a_s + f$, or 0.1812 m . The outer core, or total volume (V_o), which incorporates both the inner core and the plumage volume, is

$$V_o = V_i + V_p. \quad (6)$$

The V_o was calculated using the outer core semiaxes in equation (2): $V_o = 5.034 \times 10^{-3} \text{ m}^3$. The V_p was found by subtraction of the inner ellipsoid from the outer ellipsoid:

$$V_p = V_o - V_i = 7.23 \times 10^{-4} \text{ m}^3. \quad (7)$$

Because V_p has proven difficult to measure accurately (Stephenson 1993), the calculated V_p was compared to an empirical regression equation (Lovvorn and Jones 1991) derived from duck (Anatidae) V_p measurements (Dehner 1946; Lovvorn and Jones 1991). The equation $V_p = 0.2478 + 0.123 M_b$ for ducks gives $7.40 \times 10^{-4} \text{ m}^3$ for the Adelie penguin, which is only 2.3% higher than the value of V_p estimated above. It should be noted that largest body mass used to produce the equation for ducks was 1.2 kg , and so the Adelie penguin data point represents roughly a threefold extrapolation.

The only measurement to date of the loss of air trapped in plumage was in an ingenious experiment by Stephenson (1995), in which approximately half the air escaped the plumage of lesser scaup (*Aythya affinis*) during diving. Assuming no loss of air is therefore conservative because any reduction in air volume (including underwater exhalation) will lower buoyancy, parasite drag, and correspondingly the DMR(d).

Body Volume at Depth

The change in V_b resulting from hydrostatic compression with depth follows the Archimedes Principle and Boyle's Law (the product of gas volume and pressure is a constant). Assuming that no gas is lost during a dive, the gas volume decreases as an inverse hyperbolic function of depth, affecting the total body volume:

$$V(d) = \frac{P_s(V_R + V_p)}{P_s + P_s \left[d \left/ \frac{10329.561}{\rho} \right. \right]} + V_b, \quad (8)$$

where P_s is atmospheric pressure at the surface (101.3 kPa), ρ is seawater density (kg m^{-3}), the constant is one standard atmosphere (ATM, in kg m^{-2}), and d is depth (m).

Net Buoyancy at Depth

Net buoyant force at depth is the difference between the buoyant force (first term in eq. [9]) and the gravitational force (the second term):

$$B_{\text{net}}(d) = \rho g V(d) - g M_b. \quad (9)$$

Table 1: Oxygen reserves for diving in Adelie penguin

Oxygen reserves	Value	Study
Grand total oxygen reserve (VO_{2T})	217 mL (100%)	
Total blood oxygen	85 mL (39%)	
Arterial blood volume	124 mL	Chappell et al. 1993a
Venous blood volume	322 mL	Chappell et al. 1993a
Mean hemoglobin concentration	.187 g mL ⁻¹	Lenfant et al. 1969; Chappell et al. 1993a
O ₂ binding capacity of hemoglobin ^a	1.356 mL O ₂ g ⁻¹ Hb	Lenfant et al. 1969
O ₂ saturation of arterial blood	100%	Rothe 1983; Stephenson et al. 1989b
O ₂ saturation of venous blood	70%	Rothe 1983; Stephenson et al. 1989b
Usable proportion of blood O ₂	96%	Hudson and Jones 1986
Total muscle oxygen	59 mL (27%)	
Body mass	4 kg	Bannasch 1995
Muscle fraction of body mass ^b	35%	Chappell et al. 1993a
Myoglobin fraction of wet muscle mass	3.6% g ⁻¹	Mill and Baldwin 1983
O ₂ binding capacity of myoglobin	1.24 mL O ₂ g ⁻¹ Mb	Stephenson et al. 1989b
Myoglobin saturation	95%	Stephenson et al. 1989b
Usable proportion of muscle O ₂	99%	Stephenson et al. 1989b
Total respiratory oxygen volume (VO_{2R})	73 mL (34%)	
Total respiratory volume (V_R)	555 mL	Calder 1984
Mean fractional O ₂ concentration	17.6%	Scheid et al. 1974; Torre-Bueno 1978
Proportion of usable respiratory O ₂	75%	Hudson and Jones 1986

Note: The calculation follows Stephenson et al. (1989b) and references therein, except where noted.

^a Oxygen binding capacity 1.2 mL O₂ g⁻¹ in Viscor et al. (1984).

^b 0.25 in Stephenson et al. (1989b).

Frontal Body Area at Depth

The A_r is the area of reference to which parasite drag was compared by Bannasch (1995). Parasite drag will be scaled later with respect to change in A_r with depth, but the change in the reference area with depth is dealt with here first.

Total body volume at depth $V(d)$ can be written as the outer core ellipsoid volume at depth, $4/3 \pi a_o(d) b_o(d)^2$, where $a_o(d)$ is the outer core's ellipsoid semimajor axis length at depth and $b_o(d)$ is the corresponding semiminor axis length at depth. The change in $V(d)$ with pressure is assumed to be uniform in all three dimensions. Thus, the ratio between $b_o(d)$ and $a_o(d)$ is constant at all depths and equal to the ratio in a just-submerged bird, $a_o = 2.226b_o$, (0.1812/0.0814). Body length is likely to change less than diameter with compression. Again, equal compression is a conservative assumption because if most of the change were in the minor axis, then the cross-sectional area would decrease even faster with depth and reduce the buoyancy even more rapidly. The change in A_r as a function of depth is

$$A_r(d) = \pi \left[\frac{\sqrt[3]{V(d)}}{4/3(\pi 2.226)} \right]^2. \quad (10)$$

Basal Metabolic Rate

"On land" was chosen to represent baseline metabolism during diving: 3.6 W kg⁻¹ (Culik and Wilson 1991), or 14.4 W for a 4-kg Adelie penguin. Metabolism in the peripheral tissues decreases during the dive due to vasoconstriction and possibly cooling (Stephenson and Jones 1992; Bevan et al. 1997; Boyd 1997; Handrich et al. 1997). Thermal insulation is bound to decrease with depth as the body's insulative airspaces are compressed and heat loss by forced convection increases with swimming speed (Hind and Gurney 1997; Luna-Jorquera et al. 1997; Grémillet et al. 1998). Choosing basal metabolic rate (BMR) "on land" over the higher resting metabolic rate "on water" (Culik and Wilson 1991; Bethge et al. 1997) is closer to the expected baseline metabolic rate while diving. We conservatively assumed no decrease in BMR with depth or dive duration.

Oxygen Reserves

Adelie penguin's total O₂ reserves available for diving are 217 mL (table 1), and for the little penguin they are 56.7 mL (table 2). The calculation of the O₂ reserves follows Stephenson et al. (1989b), except when otherwise noted, and is given in detail for Adelie penguin in table 1. Differences in calculations for little penguin are itemized in "Little Penguin Model."

Table 2: Variables and parameters specific to Adelie penguin and little penguin

Symbol	Explanation	Little penguin	Adelie penguin
A	Equivalent flat plate area (m ²); eq. (19); Pennycuick 1975	3.2185×10^{-3}	.00718
A_f	Frontal body reference area (m ²) on the sea surface; see text	1.0124×10^{-2}	.02083
a	Acceleration (m s ⁻²); eq. (28)	.648	.45
a_i	"Inner core" ellipsoid semimajor axis length on the sea surface (m); eq. (5)1765
a_o	"Outer core" ellipsoid semimajor axis length on the sea surface (m); see text1812
b_i	Length of inner core ellipsoid body semiminor axis (m); see text	.052	.0765
b_o	Length of outer core ellipsoid body semiminor axis (m); eq. (4)	.057	.0814
$d_{\max, U}$	Maximum aerobic depth in a U-shaped dive profile (m)	51	72
$d_{\max, V}$	Maximum aerobic depth in a V-shaped dive profile (m)	...	54
d_{NB}	Depth at neutral buoyancy (m); online app. A, eq. (A1)	126	82
k_V	Kinematic viscosity conversion factor from 17.6°C fresh water to 10°C seawater (dimensionless)	1.246	...
k_v	Kinematic viscosity conversion factor from 17.6°C fresh water to 4°C seawater (dimensionless)	...	1.559
M_b	Body mass (kg); see text	1.2	4
S_d	Disk area (m ²); eq. (20); Pennycuick 1989	.0726	.1886
T_v	Time until constant v , acceleration phase duration (s); eq. (29)	2.8	3.3
V_i	Ellipsoid inner body core volume (m ³); eq. (3)	1.31×10^{-3}	4.324×10^{-3}
V_o	Total body volume (m ³); eq. (6)	1.705×10^{-3}	5.034×10^{-3}
V_p	Plumage volume on the sea surface (m ³); see text	3.954×10^{-4}	7.23×10^{-4}
V_R	Respiratory system volume on sea surface (m ³); eq. (1); Calder 1984	1.83×10^{-4}	5.55×10^{-4}
VO_{2P}	Pigment-bound oxygen volume (mL); see text and table 1	32.5	144
VO_{2R}	Respiratory oxygen volume (mL); see text and table 1	24.2	73
VO_{2T}	Total oxygen volume available for diving (mL); eq. (40)	56.7	217
V_b	Solid body volume (m ³); see text	1.127×10^{-3}	3.756×10^{-3}
w	Wingspan (m); see text	.304	.49

Types of Diving Profiles

Diving birds exhibit a range of diving profiles, from square-shaped U (U) dives to V-shaped dives (V; for diving profile definitions, see Schreer et al. 2001). Four parameters describe all simple dive profiles: maximum depth (d_{\max}), angle of descent, angle of ascent, and distance covered in the bottom phase.

The DMR(d) values of both V and U dive profiles are modeled here for Adelie penguin (but only the U profile for little penguin due to lack of information) because they represent the extremes in the diving profile spectrum. The U profile, characterized by vertical ascent and descent, is the shortest distance to depth and the least costly diving profile to a given depth. The V profile is the opposite in terms of distance and cost to depth, the extent depending on the actual angles of descent and ascent. The angles of descent and ascent in V profiles are assumed identical here (Wilson 1995) and are referred to as the diving angle (α , in degrees). The α exhibited by instrumented free-diving Adelie penguins is a linear positive function of the maximum depth attained in a dive (d_{\max} in eq. [11]) and is derived from figure 6.8 in Wilson 1995:

$$\alpha(d_{\max}) = 6.667 + 0.782d_{\max},$$

$$d_{\max} < 106 \text{ m}, \alpha > 0^\circ, \quad (11)$$

$$d_{\max} > 106 \text{ m}, \alpha = 90^\circ.$$

When α is less than vertical, the bird travels a longer distance than the change in depth (Δd). The actual diving distance is the product of the depth change and the ratio of the diving speed (v) to the vertical speed $\Delta d v/v_v$ ($\alpha[d_{\max}], v$). Vertical velocity is a function of $\alpha(d_{\max}, v)$ and v :

$$v_v(\alpha(d_{\max}), v) = \frac{d_{\max}}{d_{\max} \left\{ \frac{\sin[\alpha(d_{\max})]}{v} \right\}}. \quad (12)$$

Because our goal is to model the ADL(d), the duration of the bottom phase is maximized for both diving profiles, the maximum duration limit being set by the available oxygen reserves. Except when diving to the maximum aerobic depth d_{\max} , in which case the bottom time is zero, both profile types are configured to have a bottom phase.

The observed average diving speed (i.e., not horizontal

traveling speed) by Adelie penguins is 1.5 m s^{-1} (Wilson 1995; Wilson et al. 2002). After this speed is reached at the end of the acceleration phase, we assume for the sake of computational simplicity that it remains constant with depth. This is true for nonfeeding dives of Adelie penguins, but feeding dives are characterized by bursts of faster speeds (Wilson et al. 2002).

Little Penguin Model

In order to examine the applicability of the ADL to a broader range of body size, we evaluated a model for the 1.2-kg little penguin. The little penguin is an ideal candidate because it is the smallest penguin species but especially because it has been characterized to have the lowest biochemical and histochemical anaerobic capacity of penguins (Mill and Baldwin 1983; Baldwin et al. 1984; Baldwin 1988).

The little penguin's metabolic input and all metabolic output parameters are compiled as in the Adelie penguin model and multiplied by the net power efficiency (E_{net}) estimated from identical canal-respirometry data for the little penguin by Bethge et al. (1997) and provided in table 3. The general methodological outline for derived parameters follows "Basic Assumptions and Parameters" and references therein. Any differences in calculation procedures for basic parameters in the little penguin model are explained below and are itemized in table 2.

We extrapolated the relationship between frontal area and parasite drag in Adelie and Gentoo (*Pygoscelis papua*) penguins to that of the little penguin. For example, at 2.3 m s^{-1} , this extrapolation gives 0.53 N drag for the little penguin.

Because the thickness (f) of little penguin plumage is unknown, the plumage volume was estimated with Lovvorn and Jones's (1991) regression equation: $V_p = 2.478 \times 10^{-4} + 1.232 \times 10^{-4} \text{ kg body mass}$, giving $V_p = 3.956 \times 10^{-4} \text{ m}^3$ for a body mass of 1.2 kg.

Coincidentally, the estimated f (0.005 m) was the same as that found for the Adelie penguin by Kooyman et al. (1973). The f was estimated by subtracting the lengths of inner core and outer core semiminor axes (eq. [4]), each calculated from the frontal area and volume relationship (eq. [10]). One was based on the inner body core volume ($A_{f,inner} = 8.492 \times 10^{-2} \text{ m}^2$, $b_f = 0.052 \text{ m}$), and the other was based on the outer body core volume ($b_o = 0.057 \text{ m}$).

The A_f at the surface was estimated with equation (10) using the total volume and assuming that the little penguin has the same shape, that is, the ratio between the known b_o and estimated a_o axes, as in the Adelie penguin model ($a_o/b_o = 2.226$), $A_f = 1.0124 \times 10^{-2} \text{ m}^2$.

Quantitative data on little penguin diving profiles are unavailable; thus the modeled dives were assumed to be U-shaped ($d_v = S_a$ and $v_v = v$). The acceleration distance (S_a) was assumed to be 2.5 m (Wilson and Wilson 1995).

Average little penguin flipper length is 0.118 m (Williams 1995). Back width was estimated to be 0.068 m by assuming that the middle back section has the same proportion of the wingspan (w) as in the Adelie penguin (28.9%); $w \approx 0.304 \text{ m}$.

The results of five BMR studies on little penguins vary considerably, between 3.12 and 4.93 W kg^{-1} (Nicol et al. 1989). Four of these studies were done by C. D. Stahel, S. C. Nicol, and coworkers, who suggested that seasonal variation might contribute to this variability. Their lowest

Table 3: Calculation of net power efficiency (E_{net})

Variable	Adelie penguin	Little penguin
Net metabolic power input (W; $P_i - \text{BMR}$)	40.35	18.04
P_p , W at speed (m s^{-1})	54.75 (1.5); Culik et al. 1994b	21.34 (1.8); Bethge et al. 1997
BMR (W)	14.4; Culik and Wilson 1991	3.3; Nicol et al. 1989
Mechanical power output P_o , (W)	5.06	2.37
P_{par} (.5, v) k_v (W, eq. [25a])	2.52	.99
P_{ind} (.5, v) (W, eq. [21a])	.25	.12
P_{pro} (.5) (W, eq. [18a])	2.30	1.25
Average mechanical power costs of speed change ($P_a + 2P_r + P_q$)/ T_r	.47	.29
P_a (W, eq. [32])	4.50	1.94
$2P_r$ (W, eq. [31])	.94	.45
P_q (W, eq. [16])	1.12	.49
T_r (s)	14	10
Net power efficiency (E_{net} ; eqq. [15], [17])	.137	.147
Mechanical efficiency ^a	.68	.74

Note: Net power efficiency is the ratio of average metabolic input (P_i) to average net power output (P_o).

^a Assuming muscle (aerobic) efficiency of 0.2 (Hill 1950; Blake 1991).

BMR measurement ($3.3 \pm 0.70 \text{ W kg}^{-1}$) is indistinguishable from $3.12 \pm 0.1 \text{ W kg}^{-1}$ obtained by Baudinette et al. (1986). This BMR measurement was chosen to represent the little penguin baseline metabolism during diving.

The blood oxygen reserve calculation followed the outline in table 1. Blood volume was assumed to be the same fraction of body mass as in the Adelle penguin (10.15%; table 1). Little penguin mean hemoglobin blood concentration is $0.138 \text{ g Hb mL}^{-1}$ (Nicol et al. 1988), which is 73.8% of that of the Adelle penguin (table 1), and myoglobin percentage of wet muscle mass is 2.8% (Baldwin et al. 1984), which is 77.8% of the value obtained for Adelle penguins (table 1). Total blood oxygen is 18.8 mL, total muscle oxygen is 13.7 mL, and total pigment-bound oxygen is 32.5 mL. Respiratory oxygen volume was estimated to be 24.2 mL, and the total oxygen volume available for diving was $Vo_{gr} = 56.7 \text{ mL}$, or 87.1% of the Adelle penguin's mass-specific total oxygen reserve.

Components of the Depth-Dependent Diving Metabolic Rate Model

The approach taken here combines classical aeronautical theory (Pennycuik 1975, 1989) and direct laboratory measurements of parasite drag (Bannasch 1995) or extrapolations of the drag measurements to evaluate the components of mechanical power output. Metabolic power input from both species was obtained by using diving respirometry data and estimated net aerobic power efficiencies (E_{net}) obtained in artificial canals (Culik et al. 1994b; Bethge et al. 1997). The E_{net} is commonly calculated as the product of muscular (or aerobic; η_a) and mechanical (or propulsion; η_m) efficiencies (Oehme and Bannasch 1989; Stephenson et al. 1989a; Blake 1991). Muscular efficiency is the conversion rate of chemical energy to kinetic energy, and mechanic efficiency is the translation of muscle work to propulsive work. The product of the total mechanical power output and the inverse of E_{net} gives the metabolic power input needed to meet the required mechanical power output to depth, or $DMR(d)$.

When diving horizontally at constant speed, thrust equals drag, and "negative lift" equals positive buoyancy. Drag is composed of five components. First, profile drag (D_{pro}) is the backward drag of the wings and is described here using the theory of Pennycuik (1975). Second, induced drag (D_{ind}) is a negative lift force in both Adelle and little penguins' cases because they are both positively buoyant at depths less than the maximum aerobic depth attainable (d_{max} ; see app. B in the online edition of the *American Naturalist*). Hence, during descent they have to produce negative lift equal to the positive buoyancy. This is achieved by movement of water upward, the reverse of

an airborne bird in flight forcing air downward, implementing Lanchester's jet momentum theory of lift generation (Pennycuik 1989). Simply put, one can think of induced power as the power needed to sufficiently move water upward to equal the buoyancy in order to remain at depth. Third, parasite drag (D_{par}) is the frictional drag of the fuselage body. Direct measurements of parasite drag of wingless Adelle penguin (and other species) models from Bannasch (1995) are used here after extrapolating them with regard to species-specific and depth-specific differences in frontal area and correcting them for the difference in kinematic viscosity of fresh and salt water. Fourth, inertial drag is the vertical resistance to flapping the wings; however, in practice this drag cancels out and is not dealt with further (Pennycuik 1975; 1989). Fifth, the penguin has to produce metabolic power against buoyancy when descending, but when ascending, this (then negative) power aids the ascent by reducing the metabolic power input required.

Mechanical power output to depth is the sum of the power components; for example, while descending,

$$P_O(d, v) = P_{pro}(d) + P_{ind}(d, v) + kvP_{par}(d, v) + P_b(d). \quad (13)$$

The specifics of mechanical power output calculation depend on the phase of the dive, and these are portrayed in "DMR(d) Model Calculation Procedures."

Metabolic power input to depth at speed $P_i(d, v)$ equals the sum of BMR and the product of inverse net power efficiency (E_{net}) and mechanical power output to depth at speed $P_O(d, v)$:

$$P_i(d, v) = \frac{1}{K} \left\{ \frac{1}{E_{net}} P_O(d, v) + \text{BMR} \frac{\Delta d}{v_c [\alpha(d_{max}), v]} \right\}, \quad (14)$$

where the metabolic power input to depth (W) is converted into oxygen consumption (mL O_2) by multiplication with the inverse of K , the energy equivalent of 1 mL of oxygen ($K = 20.0832 \text{ J mL } O_2^{-1}$; Schmidt-Nielsen 1997).

Net Aerobic Power Efficiency

The E_{net} is calculated as the ratio of total mechanical power output (P_O) to metabolic power input (P_i) less BMR (Blake 1991):

$$E_{net} = \frac{P_O}{(P_i - \text{BMR})}. \quad (15)$$

The E_{net} was evaluated from average power input in a

still-water canal (at assumed depth of 0.5 m), as measured by Culik et al. (1994b) for Adelie penguin (see also Culik and Wilson 1991; Culik et al. 1991, 1994a) and by Bethge et al. (1997) for little penguin (see also Nicol et al. 1989). The calculations are summarized in table 3.

The bird both accelerates and decelerates during the measurement trial in the canal, and the average power requirements for the speed changes (including accelerational reaction) need to be subtracted from P_1 to obtain the net average power consumption of steady locomotion. We assume here that the E_{net} during speed change is the same as at a constant speed.

The cost of acceleration consists of two components: P_a (eq. [32]), the power needed to accelerate the body forward, and $P_r(d_v)$ (eq. [31]), which is the cost of accelerating entrained water (Daniel 1984; Vogel 1994). The cost of deceleration likewise is composed of two components: the accelerational reaction of entrained water and the body deceleration, which is assumed to be predominantly metabolically passive by "braking," guessed to be one-fourth of the acceleration power:

$$P_q = 0.25P_a. \quad (16)$$

The E_{net} is relatively insensitive to this factor; it was reduced by 4.18% and 5.2% for Adelie and little penguins, respectively, when P_q was reduced by 75% (the value used here). The other components, parasite power $P_{\text{par}}(0.5, \nu)$, induced power $P_{\text{ind}}(0.5)$, and profile power $P_{\text{pro}}(0.5, \nu)$, are calculated with equations (25), (21), and (18), respectively.

The E_{net} was calculated by iteration because it occurs on both sides of the equal sign:

$$E_{\text{net}} = \frac{P_{\text{par}}(0.5, \nu) + P_{\text{ind}}(0.5) + P_{\text{pro}}(0.5, \nu)}{P_1 - \left(\frac{1}{T_r} \times \frac{P_a + 2P_r + P_q}{T_r} \right) - \text{BMR}}, \quad (17)$$

where T_r is the time a penguin takes to swim the canal length. For Adelie penguins, the canal length was 21 m and speed was 1.5 m s^{-1} , and for little penguins, the canal length was 18 m and assumed speed was 1.8 m s^{-1} (extrapolated). The E_{net} values for Adelie and little penguins were 0.137 and 0.147, respectively (table 3).

The E_{net} is, by definition, sensitive to changes in the components of mechanical power output. For example, when plumage volume is reduced by one-half of the conservative maximum assumed here (Stephenson 1995), E_{net} becomes 0.108 for both species (implying 0.54 in mechanical efficiency, given 0.2 muscle efficiency; see table 3). Thus the apparent lowered costs of diving, by reduction in the mechanical power output, are more than counterbalanced by the resulting lesser E_{net} .

Profile Power

The P_{pro} is the rate of work against wing drag, and it decreases with depth as net buoyancy decreases (the effect of the depth-dependent decrease in A , the equivalent flat plate area of the body [eq. (19)], is conservatively ignored here). This basically reflects the reduction in wing-flapping frequency and or stroke amplitude as $B_{\text{net}}(d)$ decreases with hydrostatic compression, but diving speed is kept constant. Profile power was estimated using equation (11) from Pennycuik (1975), by replacing body mass with net buoyancy at depth. Hence during acceleration, ascent, and descent,

$$P_{\text{pro}}(d) = \frac{\nu}{\nu_r(\alpha(d_{\text{max}}), \nu)} \int_{d_i}^{d_j} \left[\frac{(X)0.877k^{0.75}B_{\text{net}}(d)^{1.5}A^{0.25}}{\rho^{0.5}S_d^{0.75}} \right] dd, \quad (18a)$$

where X is the profile power ratio (2, dimensionless), k is the induced drag factor (1.2, dimensionless), and S_d is the disk area (eq. [20]). The d_i and d_j values define the depth range (Δd) of the integral corresponding to d_0 and d_v during acceleration, to d_v and d_{max} during descent, and to d_{max} and d_0 during ascent. The P_{pro} rate in the bottom phase of the dive is

$$P_{\text{pro}}(d_{\text{max}}) = \frac{(X)0.877k^{0.75}B_{\text{net}}(d_{\text{max}})^{1.5}A^{0.25}}{\rho^{0.5}S_d^{0.75}}, \quad (18b)$$

$$A = 2.85 \times 10^{-3} M_b^{0.667}, \quad (19)$$

$$S_d = \frac{\pi w^2}{4}, \quad (20)$$

where w is the wingspan (m). The wingspan of the Adelie penguin was calculated by adding the length of each flipper (Williams 1995) to the distance between them (0.112 m), measured from figure 1b in Bannasch (1986); $w \approx 0.49 \text{ m}$.

Induced Power

When descending and swimming at the bottom at positive buoyancy, the bird has to produce a balancing negative lift. This is induced power (P_{ind}) and is assumed here to be independent of diving orientation, although when the angle of descent surpasses some stalling angle, the negative lift generation as formulated in equations (21a) and (21b) is lost. However, one can consider that P_{ind} is the cost of necessary tension maintenance against the positive buoyancy, which is independent of orientation, and that equations (21a), (21b), and (22) estimate this cost for any

descent angle. A simple explanation of P_{ind} while diving is that when the bird maintains a vertical position in the water column, it is the power needed to produce the upward movement of water in order to remain stationary (at positive buoyancy). After the lift is lost, a bird is assumed to increase its wing-flapping frequency and/or stroke amplitude to balance the induced drag and thereby to increase the speed of trailing water behind the bird by $v_i(d)$ (eq. [22]) while maintaining the same diving speed. Positive buoyancy aids the ascent, analogous to an airborne bird descending to earth under gravitational pull. The P_{ind} in this case is opposite to the upward movement of the bird, and it is the cost of displacing water to the rear of the bird. Because the calculation of P_{ind} at low speeds is unreliable (Pennycuick 1989), particularly during acceleration, it is simplistically assumed here that P_{ind} during acceleration is the same as at constant diving speed. The P_{ind} in acceleration, descent, and ascent is

$$P_{ind}(d, v) = \frac{v}{v_i(\alpha(d_{max}), v)} \int_{d_i}^{d_f} v_i(d, v) k B_{net}(d) dd, \quad (21a)$$

where $v_i(d, v)$ is the upward velocity of the water at depth (eq. [22]). The P_{ind} in the bottom phase of the dive is

$$P_{ind}(d_{max}, v) = v_i(d_{max}, v) k B_{net}(d_{max}), \quad (21b)$$

$$v_i(d, v) = \frac{B_{net}(d)}{2S_i v \rho}, \quad (22)$$

where d becomes d_{max} in the bottom phase calculation.

Parasite Power

The power exponents in Bannasch's (1995) regression equations for parasite drag for Adelie penguin, $D_{par}(v) = 0.5844v^{1.5278}$, and Gentoo penguin, $D_{par}(v) = 0.8171v^{1.5321}$ ($R^2 = 99.9\%$, $P < .001$ for both species), are virtually identical, reflecting near identical geometric shape of the two species. The difference in the intercepts, x , therefore reflects the size difference in the reference area between the species.

By assuming a linear relationship between the intercepts of the $D_{par}(v)$ equations above (x , 0.5844, and 0.8171) and the corresponding frontal body reference areas ($A_f = 0.02083$ and 0.02706 m^2) for Adelie and Gentoo penguins, respectively, and by using the average power exponent of the speed (1.53), one can extrapolate x with respect to the hydrostatically reduced reference area at depth $A_f(d)$. Accordingly, one may use the changes in body volume of Adelie penguins and the corresponding surface area with

depth, derived from Boyle's Law and elementary geometry, to extrapolate drag at any depth and speed, $D_{par}(d, v)$. It is assumed that the drag of little penguins behaves in the same fashion (i.e., solving x using $A_f = 0.010124 \text{ m}^2$ at the surface as a starting point). For either species, x is scaled as a function of frontal body area (m^2) at depth:

$$x(A_f(d)) = -0.1936 + 37.3515A_f(d). \quad (23)$$

Parasite drag at any given speed and depth is found by substituting equation (10) for $A_f(d)$ in equation (23) and inserting the resulting $x(A_f(d))$ into equation (24):

$$D_{par}(d, v) = x(A_f(d))v^{1.53}. \quad (24)$$

Bannasch's (1995) parasite drag measurements were performed in a freshwater flume at 17.6°C. To use these measurements to calculate the parasite drag in the respiratory canals and in sea conditions, one must account for the increase in kinematic viscosity ($\text{m}^2 \text{ s}^{-1}$) for the more viscous saltwater conditions. This is done by multiplying the measured parasite drag by the appropriate kinematic viscosity conversion factor ($k\nu$, dimensionless). The $k\nu$ is the ratio of the two relevant kinematic viscosities. The kinematic viscosity for each situation was linearly interpolated (table 2.1 in Vogel 1994): 17.6°C freshwater, $1.0772 \times 10^{-6} \text{ m}^2 \text{ s}^{-1}$ (flume); 4°C seawater, $1.6798 \times 10^{-6} \text{ m}^2 \text{ s}^{-1}$ (Adelie penguin's respiratory canal and sea conditions); 10°C freshwater, 1.2843×10^{-6} (little penguin respiratory canal); and 14°C seawater, $1.2843 \times 10^{-6} \text{ m}^2 \text{ s}^{-1}$ (little penguin at sea). For Adelie penguins, $k\nu = 1.559$. For little penguins, $k\nu = 1.192$ at sea and 1.216 in the respiratory canal (for the E_{net} calculation).

Parasite power to depth $P_{par}(d, v)$ in ascent and descent phases is

$$P_{par}(d, v) = k\nu \frac{v}{v_i(\alpha(d_{max}), v)} \int_{d_i}^{d_f} D_{par}(d, v) dd. \quad (25a)$$

Parasite power rate in bottom phase $P_{par}(d_{max}, v)$ is

$$P_{par}(d_{max}, v) = v D_{par}(d_{max}, v) k\nu. \quad (25b)$$

Parasite power in acceleration phase $P_{par}(d_v, v)$ is

$$P_{\text{par}}(d_v, \nu) = k\nu \frac{\nu}{\nu_v(\alpha(d_{\text{max}}), \nu)} \int_{d_0}^{d_v} x(A_i(d)) \times \left(a \sqrt{\frac{d}{0.5a}} \right)^{1.53} dd, \quad (25c)$$

where the first term in the integral is the parasite drag and the second term gives speed at depth. During constant acceleration (as assumed), instantaneous speed is equal to the product of acceleration (eq. [28]) and the time elapsed.

Buoyant Power

Boyle's Law dictates an inverse hyperbolic decrease of air volume with hydrostatic pressure, and the net buoyant force concurrently changes as an inverse hyperbolic function of depth according to equation (9). Power exerted is obtained by integrating net buoyancy: when moving against buoyancy, as in descent, $d_i = d_v$, and $d_f = d_{\text{max}}$; when supplemented by (negative) buoyancy, as in ascent, $d_i = d_{\text{max}}$, and $d_f = d_0$:

$$P_B(d) = \int_{d_i}^{d_f} B_{\text{net}}(d) dd. \quad (26)$$

DMR(d) Model Calculation Procedures

It is computationally convenient to split the calculation of total oxygen consumption into four phases: acceleration (denoted by the subscript I), descent (subscript D), bottom (subscript B), and ascent (subscript A). In the following, the calculation procedures are formulated for each phase.

Acceleration Phase

The total oxygen consumption (mL) during the acceleration phase, from the surface (d_0) to the depth when constant speed is attained (d_v ; see eq. [30]), is

$$\text{VO}_{2I} = \frac{1}{K} \left\{ \frac{1}{E_{\text{net}}} [P_a + P_i(d_v) + P_b(d_v) + P_{\text{ind}}(d_v, \nu) + P_{\text{pro}}(d_v) + P_{\text{par}}(d_v, \nu)] + T_v \text{BMR} \right\}. \quad (27)$$

It is assumed that acceleration is constant from zero to the target speed, $\nu = 1.5 \text{ m s}^{-1}$ in the Adelie penguin and

1.8 m s^{-1} in the little penguin over the distance $S_a = 2.5 \text{ m}$, as measured in African penguins (*Spheniscus demersus*; Wilson and Wilson 1995). Acceleration (m s^{-2}) is

$$a = \frac{\nu^2}{2S_a}. \quad (28)$$

The time (T_v , s) it takes to attain the target speed is the duration of the acceleration phase:

$$T_v = \frac{\nu}{a}. \quad (29)$$

The depth when constant target speed is attained (d_v , m) is

$$d_v = \sin[\alpha(d_{\text{max}})] S_a. \quad (30)$$

Acceleration reaction power was calculated using the total body volume at depth halfway down to d_v :

$$P_r(d_v) = \rho S_a V \left(\frac{d_v}{2} \right) C_a a, \quad (31)$$

where C_a is the added mass coefficient (Daniel 1984; Vogel 1994); $C_a = 0.082$ when entrained water is moving parallel to the body axis (Lamb 1932). In determining C_a , we assumed that the penguin's body shape resembles an ellipsoid where length is four times the maximal diameter (fineness ratio). Indeed, Adelie and Gentoo Penguins have fineness ratios of 4.00 and 4.35, respectively (Bannasch 1995). The actual fineness ratio of a normal little penguin is unknown, but based on body length of 0.404 m (Lovvorn et al. 2001) and the body diameter estimate (0.108 m), it is 3.74. Acceleration power is

$$P_a = a M_b S_a. \quad (32)$$

Descent Phase

The total oxygen consumption during the descent phase, from the depth when constant speed is attained ($d_v = d_i$) to maximum depth ($d_f = d_{\text{max}}$), is

$$\text{VO}_{2D} = \frac{1}{K} \left\{ \frac{1}{E_{\text{net}}} [P_B(d) + P_{\text{par}}(d, \nu) + P_{\text{ind}}(d) + P_{\text{pro}}(d, \nu)] + \text{BMR} \frac{\Delta d}{\nu_v(\alpha(d_{\text{max}}), \nu)} \right\}. \quad (33)$$

Descent time (seconds) is

$$T_D = \frac{d_{\max} - d_v}{v_v(\alpha(d_{\max}), \nu)}. \quad (34)$$

Bottom Phase

Rate of oxygen consumption (mL O₂ s⁻¹) at maximum depth is

$$\dot{V}_{O_{2B}}(d_{\max}) = \frac{1}{K} \left\{ \frac{1}{E_{\text{net}}} [P_{\text{par}}(d_{\max}, \nu) + P_{\text{ind}}(d_{\max}) + P_{\text{pro}}(d_{\max}, \nu)] + \text{BMR} \right\}. \quad (35)$$

Total oxygen consumption during the bottom phase is

$$VO_{2B} = T_B \dot{V}_{O_{2B}}(d_{\max}), \quad (36)$$

where T_B is the maximum aerobic bottom time:

$$T_B = \frac{VO_{2T} - (VO_{2I} + VO_{2D} + VO_{2A})}{\dot{V}_{O_{2B}}(d_{\max})}. \quad (37)$$

Ascent Phase

The total oxygen consumption during the ascent phase, from maximum depth (d_{\max}) to the surface (d_0), is

$$VO_{2A} = \frac{1}{K} \left\{ P_b(d) + \left[\frac{1}{E_{\text{net}}} [P_{\text{par}}(d, \nu) + P_{\text{ind}}(d) + P_{\text{pro}}(d, \nu)] + \text{BMR} \frac{\Delta d}{\nu_v} \right] \right\}. \quad (38)$$

Ascent phase duration is

$$T_A = \frac{d_{\max}}{v_v(\alpha(d_{\max}), \nu)}. \quad (39)$$

All the calculations above assume positively buoyant diving because the maximal aerobic depth attainable, d_{\max} , is less than depth at neutral buoyancy, d_{NB} (see eq. [A1] in online app. A). For Adelie penguin, $d_{NB} = 82$ m; little penguin is 126 m. If the plumage volume (V_p) is reduced by one-half, d_{NB} becomes 56 and 80 m, respectively. When $d_{\max} > d_{NB}$, the changes in equations (33) and (38) are given in online appendix B.

Model of Depth-Dependent Aerobic Diving Limit

The aerobic diving limit ADL(d) is defined here as the maximum diving time (s) to any given depth (d) at which the residual oxygen reserves (if any) will be used in the bottom phase while still allowing an aerobic return to the surface. That is, the ADL(d) estimates how long a bird can dive to any particular depth as the sum of oxygen consumption in all four phases of the dive:

$$VO_{2T} - \{VO_{2I} + VO_{2D} + [T_B \dot{V}_{O_{2B}}(d_{\max})] + VO_{2A}\} = 0, \quad (40)$$

where the sum of the oxygen consumption in each phase of the dive equals the total oxygen reserves (VO_{2T}). The maximum aerobic depth (d_{\max}) that is reachable occurs when there is no oxygen left for a bottom phase (i.e., when $T_B = 0$). The ADL as a function of depth, $tADL(d)$, is

$$tADL(d) = T_D + T_A + T_v + T_B. \quad (41)$$

Results

The components of mechanical power output (and the BMR) as functions of depth in an exemplary U-shaped diving profile of Adelie penguin to an arbitrarily chosen 60-m depth are shown in figure 1. The largest component is buoyant power, which affects the depth-specific power output the most. Parasite power increases rapidly during acceleration but remains relatively constant with depth after that. Induced power increases slightly at high buoyancy but is a small component overall. As formulated, profile power is strongly dependent on buoyancy but reaches relatively low values at depths greater than 20 m.

The instantaneous oxygen consumption at depth by an Adelie penguin, or depth-specific diving metabolic rate for the same exemplary dive as in figure 1, is given in figure 2. Including the cost of acceleration and accelerational reaction, positive buoyancy is the predominant factor of the "costly" descent. Negative buoyancy aids the ascent, as illustrated by the "down-step" at the end of bottom phase in figure 2 and, more importantly, by the overall suppression of power output during ascent. It costs ~6.8 (or $1/E_{\text{net}}$) times as much energy to offset one unit of buoyant power during descent as the buoyancy supplements during ascent (at the same respective depth).

Adelie Penguin Model

The $tADL(d)$ for both V and U diving profiles are given in figure 3, together with the corresponding bottom times.

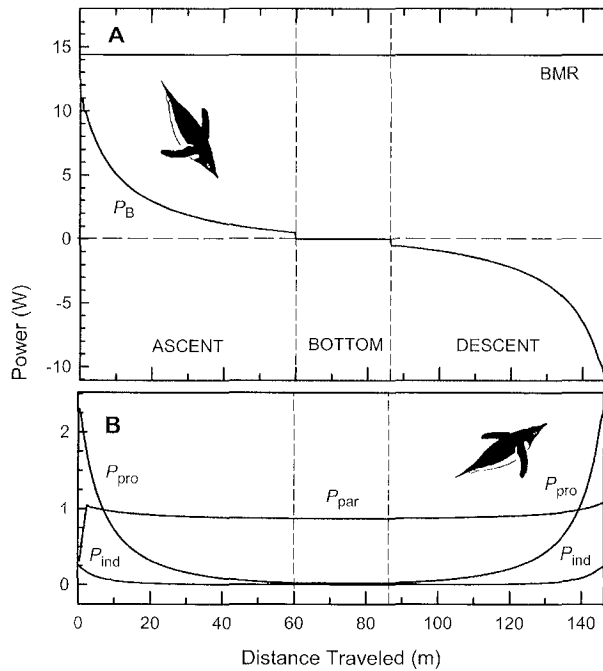


Figure 1: Instantaneous power (W) components of an exemplary U-shaped dive by the Adelle penguin, as functions of depth, to maximum depth of 60 m at diving speed of 1.5 m s⁻¹. A, Power exerted against buoyancy (positive values), power supplemented by buoyancy (negative values), and basal metabolic rate. B, Profile, parasite, and induced powers. The Adelle penguin ascends and descends vertically and swims horizontally in the bottom phase of the dive. Note that the X-axis gives the total distance traveled, and the vertical broken lines denote the beginning and end of the bottom phase (17.1 s). A color version of this figure is available in the online edition of the *American Naturalist*.

For the U-shaped profile, the maximum tADL(*d*)_U is 104.7 s (at 18-m depth), where the tADL(*d*)_U curve peaks. After their peaks, both the tADL(*d*)_U and the bottom time curves decline linearly. The maximum aerobic depth (*d*_{amax,U}) is 72 m (for a total of 98.1 s).

For the V-shaped profile, the maximum tADL(*d*)_V was 101.1 s (at 14.5-m depth), and *d*_{amax,V} was at 54 m. Bottom time decreases exponentially with depth, reflecting the increase in proportional time at depth, largely masking the opposite effect of the increase in the diving angle with depth.

The model results were compared to the most extensive data set (*n* = 14,048 dives) available on free-diving Adelle penguins (Chappell et al. 1993a): the average dive time was 73.2 ± 18.6 s (±SD), and the average dive depth was 26 ± 13 m. Using the area of the normal curve, fewer than 6.68% of all dives exceeded the model's maximum tADL(*d*)_V. It is unknown which diving profile—deep or long dives—pertains in nature. However, if we assume that Adelle penguins avoid surpassing ADL(*d*), less than 4.25%

of all dives exceed the model's maximum tADL(*d*)_U in duration, and those that do exceed the limit only slightly (see fig. 5 in Chappell et al. 1993a). Less than 1.58% of all dives exceed the model's *d*_{amax,V} and less than 0.02% exceed the model's *d*_{amax,U} (Chappell et al. 1993a). The *d*_{amax,U} = 72.3 m is 0.61 SD less the mean maximum depth of 84 ± 19 m (*n* = 20; Whitehead 1989).

Little Penguin Model

The tADL(*d*)_U is provided in figure 4 together with the corresponding bottom time, the maximum tADL(*d*)_U is 74.9 s at 15-m depth, and the maximum aerobic depth attainable (*d*_{amax,U}) is 51 m (for a total of 57.9 s).

The model's results were compared to the most extensive data set available (*n* = 6,025) of instrumented little penguins in Marion Bay, Tasmania (Bethge et al. 1997): average diving duration was 21 ± 8.4 s (±SD), and average diving depth was 3.4 ± 3.94 m. Based on the area of the normal curve, no little penguin's dives exceeded either the maximum duration or the maximum depth predicted by the model. Average maximum depth of little penguins near Phillip Island, Australia was 30 m (Montague 1984).

Discussion

The results of this exercise strongly suggest that Adelle penguins perform little anaerobic diving and that little penguins perform none whatsoever. This result is likely to

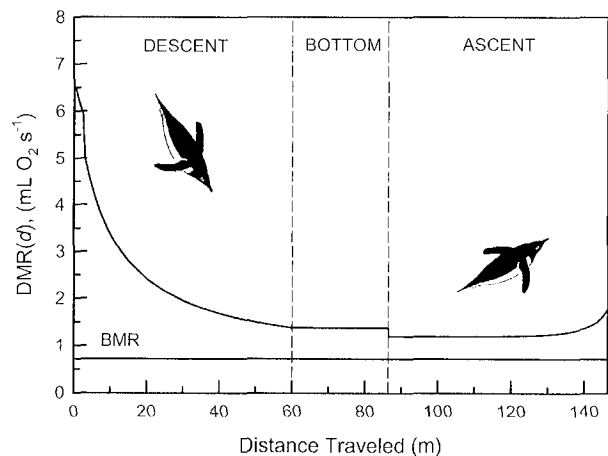


Figure 2: Adelle penguin's instantaneous diving metabolic rate (mL O₂ s⁻¹) at depth DMR(*d*)_U in an exemplary U-shaped dive to 60 m (as in fig. 1). Note that the X-axis gives the total distance traveled, and the vertical broken lines denote the beginning and end of the bottom phase (17.1 s). A color version of this figure is available in the online edition of the *American Naturalist*.

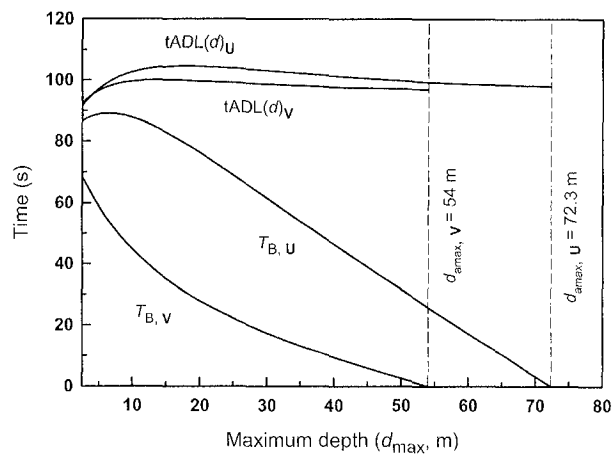


Figure 3: Depth-dependent aerobic diving limit $ADL(d)$ of Adelic penguin diving at a relative speed of 1.5 m s^{-1} . The results of two types of diving profiles are shown (denoted by the U and V subscripts). The U-shape dives are characterized by vertical descent and ascent and a horizontal "bottom phase," and the maximum $tADL(d)_U$ is 104.7 s (at 18-m depth). The V-shape dives are characterized by an increasing angle (from the horizontal) of descent and ascent, as a function of the maximal depth attained, and the maximum $tADL(d)_V$ is 101.1 s (at 14.5-m depth). Also shown is the maximal aerobic time available for the bottom phase (T_B) of a dive to a given maximum depth d_{max} , allowing for an ascent without oxygen debt. The $d_{max,U} = 72.3 \text{ m}$ (which takes 98.1 s to reach) and $d_{max,V} = 54 \text{ m}$ are the maximum aerobic depths attainable of the respective dive profiles. In comparison, the average dive time of instrumented Adelic penguins was $73.2 \pm 18.6 \text{ s}$ (mean \pm SD), and the average dive depth was $26 \pm 13 \text{ m}$ (Chappell et al. 1993a) of 14,048 dives. A color version of this figure is available in the online edition of the *American Naturalist*.

apply generally to highly positive buoyant avian deep divers and certainly not only penguins. The assumption of depth-independent (linear) DMR is not tenable for positively buoyant birds, in which case DMR is a nonlinear function of depth. It is therefore fundamentally inappropriate to calculate their ADL by linearly extrapolating measured average DMR to greater depths, which can easily produce a bias of similar magnitude as the observation (bADL) and prediction (cADL) gap. This also applies to ADL calculated by using the swimming speed at which cost of transport (J m^{-1}) is minimal (e.g., Culik et al. 1994b; Bethge et al. 1997; Luna-Jorquera and Culik 1999) because cost of transport is also depth-dependent.

The model's realism depends largely on how precisely and accurately the changes with depth can be described for the depth-dependent variables and, of course, the estimates of initial values. Although this will probably never be achieved to everybody's satisfaction (including ours), the conservative choice of the model's parameters strengthens the interpretation of the model's results. On that basis, we are confident in the main conclusion that

diving is predominantly aerobic and primarily attributable to reduction in high buoyancy while diving to depths shallower than the point of neutral buoyancy. Hypometabolism offers too small a scope of metabolism reduction to explain the large gap between observation (bADL) and prediction tADL (cf. BMR to DMR in fig. 2).

Given the observed range in the values here, reducing respiratory air volume always decreases maximum dive duration in our model because the metabolic fuel (O_2) content of a volume of air is greater than its highest buoyant carrying cost. This explains anecdotal observations that deep-diving (an arbitrary criterion of, say, $>20 \text{ m}$) birds submerge after inspiration (Kooyman et al. 1971; Stephenson et al. 1989b; Croll et al. 1992). It is a well-known fact, however, that many shallow divers submerge after expiration (Ross 1976; Livesey and Humphrey 1984; Tome and Wrubleski 1988; Lovvorn 1991). Although aerobic dives following expiration must be of shorter overall duration, they are energetically cheaper due to the reduced buoyancy; thus one would expect that highly buoyant shallow divers, that is, those experiencing proportionally the greatest costs of buoyancy, would benefit the most by diving after expiration. However, for this strategy to remain advantageous, any increase in diving frequency accompanied with the shorter dives cannot override the energetic

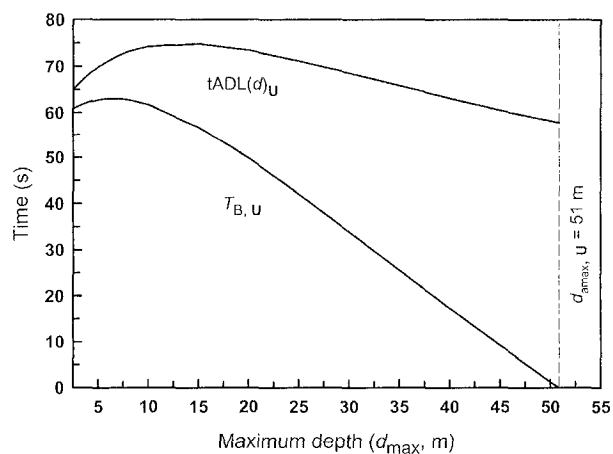


Figure 4: Depth-dependent aerobic diving limit $ADL(d)_U$ of little penguin diving at a relative speed of 1.8 m s^{-1} in a U-shaped diving profile characterized by vertical descent and ascent and a horizontal bottom phase. Also shown is the maximal aerobic time available for the bottom phase (T_B) of a dive to a given maximum depth d_{max} but allowing an ascent without inducing an oxygen debt. The maximum $tADL(d)_U$ is 74.9 s (at 15-m depth), and $d_{max,U} = 51 \text{ m}$ is the maximum aerobic depth attainable (for a total of 57.9 s). In comparison, the average dive time of instrumented little penguins was $21 \pm 8.4 \text{ s}$ (mean \pm SD, $n = 6,025$), and average diving depth was $3.4 \pm 3.94 \text{ m}$ ($n = 6,025$; Bethge et al. 1997). A color version of this figure is available in the online edition of the *American Naturalist*.

savings of shorter dives. As diving depth increases, so do the benefits of lowering the transport (buoyancy) costs of the air cargo. Indeed, birds that are not maximizing dive duration but rather minimizing the DMR by anticipating depth and dive duration should calibrate the respiratory air cargo accordingly (Keijer and Butler 1982). The aspect of optimal diving air supply is beyond the scope of this article, but for the interested, see an excellent study by Sato et al. (2002) that combines both biomechanical and experimental approaches to this problem.

There are reports where the length of diving pause on the surface between dives does increase at an accelerating rate with the length of the preceding dive (e.g., Ydenberg and Guillemette 1991; Croll et al. 1992; Kooyman and Kooyman 1995; Culik et al. 1996; Benvenuti et al. 2001; Schreer et al. 2001). But instead of invoking surpassed ADL as an explanation, one possible alternative is that digesta accumulation (Guillemette 1994, 1998) compresses the air sacs, reducing the air volume available for diving. This idea is amenable to experimentation by measuring changes in respiratory volume after incremental feedings.

Acknowledgments

Thanks to U. Hansen and B. Hardardottir for their enduring support and patience and to B. R. Hansen for invaluable help over the years. E.S.H. enjoyed a Fulbright Scholarship and a Graduate Fellowship from the University of Missouri—St. Louis while writing this article. Great thanks to all the people who reviewed and greatly improved the manuscript: A. Cohen, S. Fallon, K. Krijgsweld, J. Martinez, A. Scheuerlein, and two anonymous reviewers.

Literature Cited

- Baldwin, J. 1988. Predicting the swimming and diving behavior of penguins from muscle biochemistry. *Hydrobiologia* 165:255–261.
- Baldwin, J., J.-P. Jardel, T. Montague, and R. Tomkin. 1984. Energy metabolism in penguin swimming muscles. *Molecular Physiology* 6:33–42.
- Bannasch, R. 1986. Morphologisch-funktionelle Untersuchungen am Lokomotionsapparat der Pinguine als Grundlage für ein allgemeines Modell des "Unterwasserfluges," Teil I. Gegenbaurs morphologische Jahrbuch (Leipzig) 132:645–679.
- . 1995. Hydrodynamics of penguins: an experimental approach. Pages 141–176 in P. Dann, I. Norman, and P. Reilly, eds. *The penguins*. Surrey Beatty, Chipping Norton, New South Wales.
- Baudinette, R. V., and P. Gill. 1985. The energetics of "flying" and "paddling" in water: locomotion in penguins and ducks. *Journal of Comparative Physiology B* 155:373–380.
- Baudinette, R. V., P. Gill, and M. O'Driscoll. 1986. Energetics of the little penguin, *Eudyptula minor*: temperature regulation, the calorogenic effect of food, and moulting. *Australian Journal of Zoology* 34:35–45.
- Benvenuti, S., L. Dall'Antonia, and P. Lyngs. 2001. Foraging behavior and time allocation of chick-rearing razorbills *Alca torda* at Graesholmen, central Baltic Sea. *Ibis* 143:402–412.
- Bethge, P., S. Nicol, B. M. Culik, and R. P. Wilson. 1997. Diving behaviour and energetics in breeding little penguins (*Eudyptula minor*). *Journal of Zoology (London)* 242:483–502.
- Bevan, R. M., J. R. Speakman, and P. J. Butler. 1995. Daily energy expenditure of tufted ducks: a comparison between indirect calorimetry, doubly labelled water and heart rate. *Functional Ecology* 9:40–47.
- Bevan, R. M., I. L. Boyd, P. J. Butler, K. R. Reid, A. J. Woakes, and J. P. Croxall. 1997. Heart rates and abdominal temperatures of free-ranging South Georgian shags *Phalacrocorax georgianus*. *Journal of Experimental Biology* 200:661–675.
- Blake, R. W. 1991. On the efficiency of energy transformations in cells and animals. In R. W. Blake, ed. *Efficiency and economy in animal physiology*. Cambridge University Press, Cambridge.
- Boyd, I. L. 1997. The behavioral and physiological ecology of diving. *Trends in Ecology & Evolution* 12:213–217.
- Boyd, I. L., and J. P. Croxall. 1996. Dive durations in pinnipeds and seabirds. *Canadian Journal of Zoology* 74:1696–1705.
- Butler, P. J., and D. R. Jones. 1997. Physiology of diving of birds and mammals. *Physiological Reviews* 77:837–899.
- Butler, P. J., and A. J. Woakes. 1984. Heart rate and aerobic metabolism in Humboldt penguins, *Spheniscus humboldti*, during voluntary dives. *Journal of Experimental Biology* 108:419–428.
- Calder, W. A. 1984. *Size, function, and life history*. Harvard University Press, Cambridge, Mass.
- Chappell, M. A., V. H. Shoemaker, D. N. James, T. L. Bucher, and S. K. Mahoney. 1993a. Diving behavior during foraging in breeding Adélie penguins. *Ecology* 73:1204–1215.
- Chappell, M. A., V. H. Shoemaker, D. N. James, S. K. Mahoney, and T. L. Bucher. 1993b. Energetics of foraging in breeding Adélie penguins. *Ecology* 74:2450–2461.
- Clowater, J. S., and A. E. Burger. 1994. The diving behavior of pigeon guillemots (*Cephus columba*) off southern Vancouver Island. *Canadian Journal of Zoology* 72:863–872.
- Croll, D. A. 1990. Diving and energetics of the thick-billed

- murre, *Uria lomvia*. Ph.D. diss. University of California, San Diego.
- Croll, D. A., and E. McLaren. 1993. Diving metabolism and thermoregulation in common and thick-billed murre. *Journal of Comparative Physiology B* 163:160–166.
- Croll, D. A., A. J. Gaston, A. E. Berger, and D. Konoff. 1992. Foraging behavior and physiological adaptation for diving in thick-billed murre. *Ecology* 73:344–356.
- Culik, B. M., and R. P. Wilson. 1991. Energetics of underwater swimming in Adelie penguins (*Pygoscelis adeliae*). *Journal of Comparative Physiology B* 161:285–291.
- Culik, B. M., R. P. Wilson, R. Dannfeld, D. Adelung, H. J. Spairani, and N. R. C. Coria. 1991. Pygoscelid penguins in a swim canal. *Polar Biology* 11:277–282.
- Culik, B. M., R. Bannasch, and R. P. Wilson. 1994a. External devices on penguins: how important is shape? *Marine Biology* 118:353–357.
- Culik, B. M., R. P. Wilson, and R. Bannasch. 1994b. Underwater swimming at low energetic cost by Pygoscelid penguins. *Journal of Experimental Biology* 197:65–78.
- Culik, B. M., K. Pütz, R. P. Wilson, D. Allers, C.-A. Bost, and Y. Le Maho. 1996. Diving energetics in king penguins *Aptenodytes patagonicus*. *Journal of Experimental Biology* 199:973–983.
- Culik, B. M., G. Luna-Jorquera, H. Oyarzo, and H. Correa. 1998. Humboldt penguins monitored via VHF telemetry. *Marine Ecology Progress Series* 162:279–286.
- Daniel, T. L. 1984. Unsteady aspects of aquatic locomotion. *American Zoologist* 24:121–134.
- Davis, M. B., and H. Guderley. 1987. Energy metabolism in the locomotor muscles of the common murre (*Uria aalge*) and the Atlantic puffin (*Fratercula arctica*). *Auk* 104:733–739.
- . 1990. Biochemical adaptations to diving in the common murre, *Uria aalge*, and the Atlantic puffin, *Fratercula arctica*. *Journal of Experimental Zoology* 253:235–244.
- Davis, R. W., L. A. Fuiman, T. M. Williams, and B. J. Le Boeuf. 2001. Three-dimensional movements and swimming activity of a northern elephant seal. *Comparative Biochemistry and Physiology A* 129:759–770.
- Dehner, E. W. 1946. An analysis of buoyancy in surface-feeding and diving ducks. Ph.D. diss. Cornell University, Ithaca, N.Y.
- Falk, K., S. Benvenuti, L. Dall'Antonia, K. Kampp, and A. Ribolini. 2000. Time allocation and foraging behavior of chick-rearing Brünnich's guillemots *Uria lomvia* in high arctic Greenland. *Ibis* 142:82–92.
- Gales, R. P., C. Williams, and D. Ritz. 1990. Foraging behavior of the little penguin, *Eudyptula minor*: initial results and assessment of instrument effect. *Journal of Zoology (London)* 220:61–85.
- Grémillet, D., I. Tuschy, and M. Kierspel. 1998. Body temperature and insulation in diving great cormorants and European shags. *Functional Ecology* 12:386–394.
- Guillemette, M. 1994. Digestive-rate constraint in wintering common eiders (*Somateria mollissima*): implications for flying capabilities. *Auk* 111:900–909.
- . 1998. The effect of time and digestion constraints in common eiders while feeding and diving over blue mussel beds. *Functional Ecology* 12:123–131.
- Handrich, Y., R. M. Bevan, J.-B. Charrassin, P. J. Butler, K. Pütz, A. J. Woakes, J. Lage, and Y. Le Maho. 1997. Hypothermia in foraging king penguins. *Nature* 388:64–67.
- Hill, A. V. 1950. The dimensions of animals and their muscular dynamics. *Scientific Progress* 38:209–230.
- Hind, A. T., and W. S. C. Gurney. 1997. The metabolic cost of swimming in marine homeotherms. *Journal of Experimental Biology* 200:531–542.
- Hudson, D. M., and D. R. Jones. 1986. The influence of body mass on the endurance to restrained submergence in the Peking duck. *Journal of Experimental Biology* 120:351–367.
- Hui, C. A. 1988. Penguin swimming. II. Energetics and behavior. *Physiological Zoology* 61:344–350.
- IUPS Thermal Commission. 1987. Glossary of terms for thermal physiology. 2d ed. *Pflügers Archiv* 410:567–587.
- Keijer, E., and P. J. Butler. 1982. Volumes of the respiratory and circulatory systems in tufted and mallard ducks. *Journal of Experimental Biology* 101:213–220.
- Kooyman, G. L. 1975. Behavior and physiology of diving. Pages 115–137 in B. Stonehouse, ed. *The biology of penguins*. Macmillan, London.
- . 1989. *Diverse divers: physiology and behavior*. Zoophysiology. Vol. 23. Springer, Berlin.
- Kooyman, G. L., and T. G. Kooyman. 1995. Diving behavior of emperor penguins nurturing chicks at Coulman Island, Antarctica. *Condor* 97:536–549.
- Kooyman, G. L., C. M. Drabek, R. Elsner, and W. B. Campbell. 1971. Diving behavior of the emperor penguin, *Aptenodytes forsteri*. *Auk* 88:775–795.
- Kooyman, G. L., J. P. Schroeder, D. G. Greene, and V. A. Smith. 1973. Gas exchange in penguins during simulated dives to 30 and 68 m. *American Journal of Physiology* 225:1467–1471.
- Kooyman, G. L., M. A. Castellini, R. W. Davis, and R. E. Maue. 1983. Aerobic diving limits of immature Weddell seals. *Journal of Comparative Physiology B* 151:171–174.
- Kooyman, G. L., Y. Cherel, Y. Le Maho, J. P. Croxall, P. H. Thorson, V. Ridoux, and C. A. Kooyman. 1992. Diving behavior and energetics during foraging cycles in king penguins. *Ecological Monographs* 62:143–163.
- Kovacs, C. E., and R. A. Meyers. 2000. Anatomy and his-

- tochemistry of flight muscles in a wing-propelled diving bird, the Atlantic puffin, *Fratercula arctica*. *Journal of Morphology* 244:109–125.
- Lamb, S. H. 1932. *Hydrodynamics*. Dover, New York.
- Lenfant, C., G. L. Kooyman, R. Elsner, and C. M. Drabek. 1969. Respiratory function of the blood of the Adélie penguin. *American Journal of Physiology* 216:1598–1600.
- Livesey, B. C., and P. S. Humphrey. 1984. Diving behavior of steamer ducks *Tachyeres* spp. *Ibis* 126:257–260.
- Lovvorn, J. R. 1991. Mechanics of underwater swimming in foot-propelled diving birds. *Proceedings of the International Ornithological Congress* 20:1868–1874.
- Lovvorn, J. R., and D. R. Jones. 1991. Effects of body size, body fat and change in pressure with depth on buoyancy and costs of diving in ducks (*Aythya* spp.). *Canadian Journal of Zoology* 69:2879–2887.
- Lovvorn, J. R., D. A. Croll, and G. A. Liggins. 1999. Mechanical versus physiological determinants of swimming speeds in diving Brünnich's guillemots. *Journal of Experimental Biology* 202:1741–1752.
- Lovvorn, J. R., G. A. Liggins, M. H. Borstad, S. M. Calisal, and J. Mikkelsen. 2001. Hydrodynamical drag of diving birds: effects of body size, body shape and feathers at steady speeds. *Journal of Experimental Biology* 204:1547–1557.
- Luna-Jorquera, G., and B. M. Culik. 1999. Diving behavior of Humboldt penguins *Spheniscus humboldti* in northern Chile. *Marine Ornithology* 27:67–76.
- . 2000. Metabolic rates of swimming Humboldt penguins. *Marine Ecology Progress Series* 203:301–309.
- Luna-Jorquera, G., R. P. Wilson, B. M. Culik, R. Aguilar, and C. Guerra. 1997. Observations of the thermal conductance of the Adélie (*Pygoscelis adeliae*) and Humboldt (*Spheniscus humboldti*) penguins. *Polar Biology* 17:69–73.
- Mahoney, S. A. 1984. Plumage wettability in aquatic birds. *Auk* 101:181–185.
- Mill, G. K., and J. Baldwin. 1983. Biochemical correlates of swimming and diving behavior in the little penguin *Eudyptula minor*. *Physiological Zoology* 56:242–254.
- Montague, T. 1984. A maximum dive recorder for little penguins. *Emu* 85:264–267.
- Nagy, K. A., W. R. Siegfried, and R. P. Wilson. 1984. Energy utilization by free-ranging jackass penguins, *Spheniscus demersus*. *Ecology* 65:1648–1655.
- Nicol, S. C., W. D. Melrose, and C. D. Stahel. 1988. Haematology and metabolism of the blood of the little penguin, *Eudyptula minor*. *Comparative Biochemistry and Physiology A* 89:383–386.
- Nicol, S. C., C. D. Stahel, U. Mesch, and N. A. Andersen. 1989. Thermoregulation in the little penguin, *Eudyptula minor*. Pages 691–695 in J. B. Mercer, ed. *Thermal physiology*. Elsevier, Berlin.
- Nowacek, D. P., M. P. Johnson, P. L. Tyack, K. A. Shorter, W. A. McLellan, and D. A. Pabst. 2001. Buoyant ballenids: the ups and downs of buoyancy in right whales. *Proceedings of the Royal Society of London Series B* 268:1811–1816.
- Oehme, H., and R. Bannasch. 1989. Energetics of locomotion in penguins. Pages 230–240 in W. Wieser and E. Gnaiger, eds. *Energy transformation in cells and organisms*. Thieme, Stuttgart.
- Pennyquick, C. J. 1975. Mechanics of flight. Pages 1–75 in D. S. Farner and J. R. King, eds. *Avian biology*. Academic Press, New York.
- . 1989. *Bird flight performance: a practical calculation manual*. Oxford University Press, Oxford.
- Ponganis, P. J., G. L. Kooyman, and M. A. Castellini. 1993. Determinants of the aerobic dive limit of Weddell seals: analysis of diving metabolic rates, postdive end tidal PO_2 's, blood and muscle oxygen stores. *Physiological Zoology* 66:732–749.
- Ponganis, P. J., G. L. Kooyman, L. N. Starke, C. A. Kooyman, and T. G. Kooyman. 1997. Postdive blood lactate concentrations in emperor penguins, *Aptenodytes forsteri*. *Journal of Experimental Biology* 200:1623–1626.
- Ross, R. K. 1976. Notes on the behavior of captive great cormorants. *Wilson Bulletin* 88:143–145.
- Rothe, C. E. 1983. Venous system: physiology of the capacitance vessels. Pages 397–452 in J. T. Shepherd and F. M. Abboud, eds. *Handbook of physiology: the cardiovascular system*. American Physiological Society, Bethesda, Md.
- Sato, K., Y. Naito, A. Kato, Y. Niizuma, Y. Watanuki, J.-B. Charrassin, C.-A. Bost, Y. Handrich, and Y. Le Maho. 2002. Buoyancy and maximal diving depth in penguins: do they control inhaling air volume? *Journal of Experimental Biology* 205:1189–1197.
- Scheid, P., H. Slama, and H. Willmer. 1974. Volume and ventilation of air sacs in ducks studied by inert gas washout. *Respiration Physiology* 21:19–36.
- Schmidt-Nielsen, K. 1997. *Animal physiology: adaptation and environment*. Cambridge University Press, Cambridge.
- Schreer, J. F., K. M. Kovacs, and R. J. O. H. Hines. 2001. Comparative diving patterns of pinnipeds and seabirds. *Ecological Monographs* 71:137–162.
- Skrovan, R. C., T. M. Williams, P. S. Berry, P. W. Moore, and R. W. Davis. 1999. The diving physiology of bottlenose dolphins (*Tursiops truncatus*). II. Biomechanics and changes in buoyancy at depth. *Journal of Experimental Biology* 202:2749–2761.
- Stephenson, R. 1993. The contributions of body tissues,

- respiratory system and plumage to buoyancy in waterfowl. *Canadian Journal of Zoology* 71:1521–1529.
- . 1995. Respiratory and plumage gas volumes in unrestrained diving ducks (*Aythya affinis*). *Respiration Physiology* 100:129–137.
- Stephenson, R., and C. A. Andrews. 1997. Wettability in aquatic birds. *Canadian Journal of Zoology* 74:288–294.
- Stephenson, R., and D. R. Jones. 1992. Blood flow distribution in submerged and surface-swimming ducks. *Journal of Experimental Biology* 166:285–296.
- Stephenson, R., J. R. Lovvorn, M. R. A. Heieis, D. R. Jones, and R. W. Blake. 1989a. A hydromechanical estimate of the power requirements of diving and surface-swimming in lesser scaup (*Aythya affinis*). *Journal of Experimental Biology* 147:507–519.
- Stephenson, R., A. K. Turner, and P. J. Butler. 1989b. The relationship between diving activity and oxygen storage capacity in the tufted duck (*Aythya fuligula*). *Journal of Experimental Biology* 141:265–275.
- Stephenson, R., M. S. Hedrick, and D. R. Jones. 1992. Cardiovascular responses to diving and involuntary submergence in the rhinoceros auklet (*Cerorhinca monocerata* Pallas). *Canadian Journal of Zoology* 70:2303–2310.
- Tome, M. W., and D. A. Wrubleski. 1988. Underwater foraging behavior of canvasbacks, lesser scaups, and ruddy ducks. *Condor* 90:168–172.
- Torre-Bueno, J. R. 1978. Respiration during flight in birds. Pages 89–94 in J. Piiper, ed. *Respiratory function in birds, adult and embryonic*. Springer, Berlin.
- UNESCO. 1987. International oceanographic tables. UNESCO Technical Papers in Marine Science 40 4:1–195.
- Viscor, G., J. Fuentes, and J. Palomeque. 1984. Blood rheology of the pigeon (*Columba livia*), hen (*Gallus domesticus*), and black-headed gull (*Larus ridibundus*). *Canadian Journal of Zoology* 62:2150–2156.
- Vogel, S. 1994. *Life in moving fluids: the physical biology of flow*. Princeton University Press, Princeton, N.J.
- Webb, P. M., D. E. Crocker, S. B. Blackwell, D. P. Costa, and B. J. Le Boeuf. 1998. Effects of buoyancy on the diving behavior of northern elephant seals. *Journal of Experimental Biology* 201:2349–2358.
- Whitehead, M. D. 1989. Maximum diving depths of the Adélie penguin, *Pygoscelis adeliae*, during the chick rearing period in Pridz Bay, Antarctica. *Polar Biology* 9:329–332.
- Williams, T. D. 1995. *The penguins: bird families of the world*. Vol. 2. Oxford University Press, Oxford.
- Williams, T. M., R. W. Davis, L. A. Fuiman, J. Francis, B. J. Le Boeuf, M. Horning, J. Calambokidis, and D. A. Croll. 2000. Sink or swim: strategies for cost-efficient diving by marine mammals. *Science* 288:133–136.
- Wilson, R. P. 1995. Foraging ecology. Pages 81–106 in T. D. Williams, ed. *The penguins: bird families of the world*. Vol. 2. Oxford University Press, Oxford.
- Wilson, R. P., and D. Grémillet. 1996. Body temperatures of free-living African penguins (*Spheniscus demersus*) and bank cormorants (*Phalacrocorax neglectus*). *Journal of Experimental Biology* 199:2215–2223.
- Wilson, R. P., and M.-P. T. Wilson. 1995. The foraging ecology of the African penguin *Spheniscus demersus*. Pages 244–265 in P. Dann, I. Norman, and P. Reilly, eds. *The penguins*. Surrey Beatty, Chipping Norton, New South Wales.
- Wilson, R. P., K. Hustler, P. G. Ryan, A. E. Burger, and E. C. Nöldeke. 1992. Diving birds in cold water: do Archimedes and Boyle determine energetic costs? *American Naturalist* 140:179–200.
- Wilson, R. P., Y. Ropert-Coudert, and A. Kato. 2002. Rush and grab strategies in foraging marine endotherms: the case for haste in penguins. *Animal Behaviour* 63:85–95.
- Ydenberg, R. C., and M. Guillemette. 1991. Diving and foraging in the common eider. *Ornis Scandinavica* 22:349–352.

Associate Editor: Peter C. Wainwright